Oral Pyruvate Protection of Dorsal Root Ganglia in Simulated Weightlessness Rats

Yuan Li
Chinese PLA General Hospital
Heng Zhang
Chinese PLA General Hospital
Ning-Tao Ren
Chinese PLA General Hospital
Chao Chen
Chinese PLA General Hospital
Peng Qi
Chinese PLA General Hospital
Fang-Qiang Zhou (fqzh60130@yahoo.com)
Shanghai Sandai Pharmaceutical R&D Co., Ltd https://orcid.org/0000-0003-1967-6943
Geng Cui
Chinese PLA General Hospital

Research article

Keywords: Dorsal root ganglia, Glial cell line-derived neurotrophic factor, Glial fibrillary acidic protein, Hindlimb unweighting, Neuron, Pyruvate

Posted Date: June 4th, 2020

DOI: https://doi.org/10.21203/rs.3.rs-32550/v1

Abstract

Background: Previous studies demonstrate that long-tern microgravity induces multi-organ injury and dysfunction, including the dorsal root ganglia (DRG) damage. This study investigated oral pyruvate protective effects on lumbar 5 (L5) DRG nerve tissues in rats subjected to hindlimb unweighting (HU).

Results: Male Sprague-Dawley rats were randomly assigned to four groups (n=10): control group (Group CON), suspension group (Group SUS), normal saline group (Group SAL) and sodium pyruvate group (Group PYR), respectively. The rats of SUS, SAL and PYR groups were simulated with microgravity by tail suspension of HU for 8 weeks. Rats in Groups SAL and PYR fed with normal saline and pyruvate saline, respectively. Histopathological and immunofluorescence examinations were conducted and levels of glial cell line-derived neurotrophic factor (GDNF), glial fibrillary acidic protein (GFAP), ATP and ATPase were measured in DRG tissues; L5 spinal cord scans were also carried out in rats following HU. Results showed that the HU resulted in significant alterations in DRG nerve tissues' structure and function in Groups SUS and SAL, whereas morphological changes were not significantly distinguished between Group PYR and Group CON; GDNF, GFAP, ATP and ATPase levels were mostly preserved in Group PYR, but still worse than in Group CON. The significance of oral pyruvate protection against DRG injury following HU and the dose and formula of oral pyruvate solutions were discussed for use in astronauts' spaceflight.

Conclusions: oral pyruvate effectively protected L5 DRG from pathological alterations and dysfunction induced by the HU in rats. Further studies and clinical trials are warranted.

Background

The status of astronauts' health and safety in space exploration missions is a very important issue. When they enter the space environment, astronauts' physiological functions are affected in various facets, such as negative calcium balance, muscle atrophy and bone loss, cardiovascular and immune system disorders, brain and spinal cord injury (SCI) and so on [1-5] And several interventions for these disturbances were proposed [6,7].

Dorsal root ganglion (DRG) is a critical anatomical structure involved in stimulating sensation of pain injury. It is also an important synthetic site of neurotrophic factors and neurotransmitters, which play a pivotal role in the nutrition and injury repair of nerves. Under simulated weightlessness, the expression of neurotrophic factors and genomics is altered and the degenerative alteration of myelin sheath appears in the fifth lumbar spine (L5) DRG in rats. These aberrances reflect its damage from the microscopic point of view [5,8].

Pyruvate is the intermediate product of glycolysis at the junction of glucose anaerobic and aerobic metabolism. It is the metabolic hub of the three major nutrients, not only an energy substrate, but also an anti-oxidative stress and anti-inflammatory agent. Pyruvate holds several superior physiological and pharmacological characteristics in comprehensive improvement of glucometabolic disturbances and protection of mitochondrial function, so that it is multi-organ protective against noxious stimuli [9-11].

Several reports have evidenced that pyruvate has protective function against damage of brain and nerve tissues caused by various pathological insults [8,9,12]. Further, recent findings indicated that enteral pyruvate in a pyruvate-enriched oral rehydration solution (Pyr-ORS) profoundly preserved neurons structure and function following ashyxial cardiac arrest in rats [13].

Based on our prior observation [8], the present study aims to investigate the effect of oral sodium pyruvate solution on the DRG injury, by highlight of the changes in morphological structure and metabolic function of DRG nervous cells, in rats subjected with simulated weightlessness and provides the first experimental evidence for oral pyruvate in prevention and treatment of the back pain and beyond in astronauts' spaceflight.

Materials And Methods

Animal and tissue treatment

Forty 3-month old, male, Sprague-Dawley (SD) rats ( ), purchased from the Animal Experimental Center of the Academy of Military Medical Sciences, Beijing, were divided into 4 groups ( ): control group (Group CON), suspension group (Group SUS), normal saline group (Group SAL) and sodium pyruvate saline group (Group PYR). The design procedures were following previous findings [8]. The rats of Groups SUS, SAL and PYR were simulated with microgravity effects by the tail suspension of hindlimb unweighting (HU) model [8]. The hind limbs (legs) of the rats were held off the horizontal plane approximately at a 30° angle. Rats in the CON and SUS groups were fed with conventional laboratory water. The rats of Group SAL and Group PYR were orally given with 0.9% sodium chloride solution (normal saline, NS, [Na^+] 154 mmol/L, [Cl^-]) and sodium pyruvate saline daily to replace the conventional laboratory water, respectively. Pyruvate saline was prepared in the laboratory on the basis of the patent (Patent No.: US 8,835,508 B2) formula: ([Na^+] 154 mmol/L, [Cl^-]) and [Pyr^-]). The total volume of drinking water fed daily was about in each rat.

The rats were housed in cages (2-3 in each) with experimental wood chip bedding and placed in a 12-hour light/dark cycle in the similar conditions during experimentation with standard laboratory food and light, as previously conducted [8]. After 1 week of adaptive suspension, the experimental rats with hindlimb unweighting lasted 8 weeks. At the end of the experiment, the rats were euthanized by intraperitoneal injection of sodium pentobarbital with a lethal dose ( ) and dissected. The rats' lumbar 5 dorsal root ganglia (L5 DRG in both sides each rat) were quickly excised, frozen in the isopentane cooled with liquid nitrogen [8]. Normal saline (Cisen Pharmaceutical Co., China) was obtained from the Animal Laboratory of PLA General Hospital and sodium pyruvate was purchased from Sigma Co. (St Louis, MO).

Hematoxylin-Eosin staining (HE) and toluidine blue staining

As described before [8], the DRG tissue samples were fixed in formalin for 24 hours, washed and dehydrated by ethanol gradient. Then, tissue blocks were embedded in conventional paraffin, treated with

dimethyl benzene and finally sliced in sections. The sections were incubated at 60℃ for 1 hour and then dewaxed with xylene, dehydrated with ethanol and stained with hematoxylin and eosin.

For toluidine blue staining, the sections of DRG were placed on the coverslips, washed by phosphate buffered saline (PBS) and fixed in 4% paraformaldehyde for 30 minutes and stained with 1% toluidine blue at room temperature for 30 minutes. The sections then were washed with absolute ethanol, dried, cleared and finally coverslipped. Tissue sections were analyzed by a light microscopy (400X, OLYMPUS BX46). The researchers were blinded to observe the experimental samples. The quantity of Nissl-stained neurons per 1 mm^2 region of the five random areas was counted in average by using an optical microscopy and the ImageJ tool software (Nikon NIS-Elements, USA).

Western blot analysis

As previously described, the DRG tissues were prepared for Western Blotting [8,14]. Briefly, total proteins of DRG were extracted by standard methods and the protein content was determined by the Bradford method. The cell lysate separated by using SDS-PAGE and then transferred to the PVDF membrane. All membranes were blocked in TBST contained 5% skim milk for 30 minutes at room temperature, followed by incubation with the primary antibody (1:1000, rabbit anti-rat GDNF [ab64337, Abcam]; 1:1000, rabbit anti-rat GFAP [ab138701, Abcam] and 1:5000, anti-β-actin [ab95437, Abcam]) overnight at 4℃, respectively. Blots were washed with TBST and incubated in secondary antibodies (goat anti-rabbit IgG [1:2000, Abcam]) for 1 h at 37℃. The protein expression was visualized with enhanced chemiluminescence (ECL) reagents (Amersham, Cleveland, OH, USA) and the membranes were exposed to Hyperfilm (Amersham). The intensity values of glial cell-derived neurotrophic factor (GDNF) and glial fibrillary acidic protein (GFAP) were determined with the Quantity-One software (BIO-RAD, USA) and each group was compared with β-chain. The results for the two proteins were expressed in relative ratios, respectively.

Spinal Cord Scan

All SD rats, before sacrifices, were pre-anesthetized in the pre-anesthetic box (ABM, Yuyan Instruments Co. Ltd., China) with an anesthetic dose of 5cps and oxygen of 2lps. After rats were deeply anesthetized (both eyes closed without reaction by shaking the anesthesia box) for 2 minutes, rats were moved into the magnet and fixed head to a magnetic resonance imaging (MRI) lift bed with a prostrate position, as previously reported [15]. With continuous anesthesia (2% isoflurane gas), all rats were fixed with the head advanced and prone position. After the fixation was completed, continuous anesthesia was performed in a group sequence. Ensured the connection was correct to keep rats' condition monitored during the inspection process in L5, a fast spin echo (FSE) sequence PDWI is used to scan the region of interest (ROI) across sections, sagittal surfaces and coronal surfaces. Scan parameters were repetition time: 2000 ms; echo time: 28 ms, scan layer: 24 layers, field of view: ; number of signal average: 15; scan time: 5 min 50 ms, using the small animal NMR instrument GE Signa Excite 0.35T scanner. Using the ImageJ tool

software (Nikon NIS-Elements, USA) to calculate the relative area ratio of the gray matter in four groups with Group CON as 1.0.

Tissue ATP content

The L5 DRG tissue in each rat was quickly homogenized to prepare the tissue lysate and the protein concentration was determined. ATP levels in DRG tissues were measured with absorbance values, as previously reported [16]. The tissue ATP content was determined stringently following the procedures provided by the test kit purchased from Nanjing Jiancheng Bioengineering Institute, China. Finally, the absorbance values at 636 nm were read with each tube by HPLC (high performance liquid chromatograph, Agilent CO., USA). The ATP content of the test sample was calculated, according to the following formula:

ATP content (nmol/gprot) = (test tube-control tube) / (standard tube-blank tube) × standard content × dilution times ÷ protein (gprot/L)

Tissue ATPase activity

In strict accordance with the ATPase test kit instructions (SuZhou Comin Biotechnology Co., Ltd, China), L5 DRG tissues were accurately weighed and the weight over volume ratio of 1:9 was obtained by adding 0.9% sodium chloride solution to make enzyme solution samples. Samples were homogenized and centrifuged at 2000rpm at 4℃for 10 minutes. The supernatant 0.2 mL were diluted to homogenate with 0.9% sodium chloride 0.8 ml. Then, enzymatic and phosphorylation reactions were performed according to the operation table in the test kit. Finally, the amount of inorganic phosphoric acid was calculated by colorimetric determination at 660 nm (Agilent CO., USA). The ATPase activity was calculated according to the following formula:

ATPase activity (μmol/mgprot/h) = (test tube-control tube) / (standard tube-blank tube) × standard content × dilution times × 6 ÷ protein (mgprot/ml)

Myelin sheath immunofluorescence

As previously described [17] for immunofluorescence detection to identify the expression of myelin sheath, a continuous cross section of a 20-μm thick L5 DRG tissue was produced by cryostat (Microm, Heidelberg, Germany). The sections were thawed at room temperature for 30 minutes for staining. The tissues were washed with PBS and then incubated with 3% hydrogen peroxide for 10 minutes. Next, sections were rinsed by normal goat serum at room temperature for 2 hours and incubated with polyclonal degenerated myelin basic protein (dgen-MBP) primary antibody (1:1000, Chemicon Inc., Temecula, USA) overnight at 4℃. After rinsing, the sections were incubated at 4℃ overnight with a secondary antibody (1:200, donkey anti-rabbit IgG-FITC; Jackson ImmunoResearch Laboratories Inc., West Grove, PA, USA). Then, sections were washed three times with PBS for 10 minutes each time. Finally, the sections were mounted by using Floursave mounting reagent (Cal Biochem, La Jolla, USA). Comparisons among groups were made based on stained area and mean optical density (OD). Images

were collected and the mean OD value was quantified using ImageJ software (National institute of Health, USA).

Data analysis

The SPSS 17.0 software was used for statistical analyses of data expressed as mean ± SD. Comparison of data among four groups were analyzed, using the Student's t test. One-way analysis of variance test was used to calculate significance among the various groups. Statistically significant was defined as $P < 0.05$.

Results

Effects of pyruvate on cell morphology and Nissl bodies in L5 DRG tissues

HE staining

In the PYR group, the DRG nervous cells showed only mild swelling and a small amount of cytoplasm vacuoles. In contrast, in the SUS and SAL groups, the DRG cells presented quite swelling, gap widened in varying degrees and some cytoplasmic vacuoles and numerous fine granular basophilic materials among cells.

These changes appeared more significant in the SUS and SAL groups than in the CON and PYR groups. The cell morphological appearance in Group PYR was slightly changed in comparison with that in Group CON (Fig. 1).

In the PYR group, the DRG neurons showed only mild swelling and a small amount of cytoplasm vacuoles. In the SUS and SAL groups, the neurons presented quite swelling, gap widened in varying degrees and some cytoplasmic vacuoles and there were numerous fine granular basophilic materials among the cells. The cell morphological appearance in Group PYR was slightly changed in comparison with that in Group CON (scale bars 25μm).

Nissl body in neuron

In the CON and PYR groups, Nissl basophilic granules were abundant with near normal appearances in neurons. However, in the SUS and SAL groups, the morphological size and the distribution pattern of Nissl bodies were smaller and scattered, which were lightly stained. In some DRG cells, the Nissl bodies also appeared disassociated. In addition, the observed and quantified changes were more significant in the SUS and SAL groups than in the CON and PYR groups and there was no significant difference in numbers of Nissl body stained neurons between Groups CON and PYR (Fig. 2 A and B).

In the CON and PYR groups, Nissl basophilic granules were abundant with near normal appearance. However, in the SUS and SAL groups, the Nissl bodies were lightly stained with smaller morphological

sizes and scattered distribution. In some DRG neurons, the Nissl bodies also appeared disassociated in Groups SUS and SAL (scale bars 100μm).

The amounts of Nissl-stained neurons/1.0 mm^2 in five random fields were quantified by using a light microscope (X400; five section slices were evaluated in average in each rat; n = 10). In addition, the observed and quantified changes were more obvious in the SUS and SAL groups than in the CON and PYR groups and there was no significant difference in numbers of Nissl body staining neurons between Groups CON and PYR. There were statistically significant differences between Groups SUS and SAL from Group PYR, respectively (**P<0.01).

Degenerated-MBP expression

In the SUS and SAL groups, the cell number of dgen-MBP was increased; the cells were swollen and their boundaries were unclear with heavy fluorescent in the immunofluorescence detection. These changes did not obviously appear in the CON and PYR groups (Fig. 3 A). The mean OD value of dgen-MBP was significantly increased in Groups SUS and SAL, compared with Groups CON and PYR. As shown in Fig. 3 B, there were statistically significant differences between Groups SUS and SAL from Groups CON and PYR (P<0.01), however, there was no difference between both later groups (P>0.05) in the mean OD value.

The SUS and SAL groups showed more expressions of dgen-MBP than the CON and PYR groups (scale bars 50μm).

Mean OD values of dgen-MBP immunofluorescence staining in L5 DRG were higher in Groups SUS and SAL than in Groups CON and PYR. There were statistically significant differences between Groups SUS and SAL from Group PYR, respectively (**P<0.01).

dgen-MBP: degenerated myelin basic protein

Spinal cord scan

In the CON groups, the gray matter and white matter areas in L5 were normal. In the SUS and SAL groups, the areas of gray matter and white matter were atrophy. These alterations appeared more significant in the SUS and SAL groups than in the PYR group that was close to Group CON. The relative area ratios of gray matter in the HU groups to the CON group also illustrated a significant decrease in Groups SUS and SAL, but a comparable outcome in Groups PYR and CON (Fig. 4 A and B).

In Group CON and PYR, the posterior part of the gray matter dorsal horn was slightly thicker and the outer layer was gentle; the edge of the anterior horn of the gray matter was enlarged and smooth. In Group SUS

and SAL, the middle and lateral parts of the gray matter dorsal horn were slightly curved and the out layer was steep. In Group SUS, the medial margin of the anterior horn was thinner; in Group SAL, the anterior horn of the gray matter was significantly reduced (scale bars 1μm).

The gray matter area was bigger in the PYR group than in the SUS and SAL groups. The alterations appeared more significant in the SUS and SAL groups than in the CON and PYR groups and they were close to each other in Groups CON and PYR. The gray matter areas were statistically significant differences between SUS and SAL from PYR groups, respectively (**P<0.01).

Effects of pyruvate on GDNF and GFAP expressions in L5 DRG tissues

GDNF protein

As shown in Fig. 5, 8 weeks of simulated microgravity induced a significant reduction in GDNF expressions. Compared with the CON group, the relative GDNF protein content in the DRG was reduced by 21% and 20% in the SUS and SAL groups, respectively. In contrast, the GDNF content was 123% and 112% higher in the PYR group than in the SUS and SAL groups, respectively. There were statistically significant differences between SUA and SAL groups from CON and PYR groups (P<0.01). However, the protein content was significantly higher in group PYR than in group CON (p<0.01).

Simulated microgravity induced significant reduction in GDNF expressions. There were statistically significant differences between SUA and SAL groups from CON and PYR groups. However, the protein content was significantly higher in Group PYR than in Group CON. There were statistically significant differences between Groups CON, SUS and SAL from Group PYR, respectively (**P<0.01).

GFAP expression

The relative GFAP protein expression was significantly increased in all three suspension groups, compared with Group CON, as shown in Fig. 6. GFAP contents were 2.5 times and 2.3 times in Groups SUS and SAL over Group CON, respectively. However, the GFAP protein in Group PYR was reduced by 28% and 24%, compared to Groups SUS and SAL, respectively. There were statistically significant differences between Groups SUA and SAL from Groups CON and PYR (P<0.01). And the GFAP level was still significantly higher in Group PYR than in Group CON (P< 0.01).

The GFAP protein expressions were significantly increased in all three suspension groups. There were statistically significant differences between Groups SUA and SAL from Groups CON and PYR. And the GFAP level was still significantly higher in Group PYR than in Group CON. There were statistically significant differences between CON, SUS and SAL from Group PYR, respectively (**P<0.01).

Effects of pyruvate on ATP and ATPase expressions in L5 DRG tissues

ATP content

The adenosine triphosphate (ATP) content was decreased in all three suspension groups, compared to Group CON. ATP contents (nmol/gprot) were reduced by 60% and 61% in Groups SUS and SAL from Group CON, respectively. However, they were 35% and 38% higher in the PYR group than in the SUS and SAL groups, respectively. There were statistically significant differences between Groups SUS and SAL from Groups CON and PYR ($P<0.05$; $P<0.01$; Fig. 7 A). However, the ATP level was still significantly lower in Group PYR, compared with Group CON ($P<0.01$).

The ATP contents were decreased in all three suspension groups. There were statistically significant differences between Groups SUA and SAL from Groups CON and PYR. However, the ATP level was still significantly lower in Group PYR compared with Group CON. There was a statistically significant difference between Group SUS and Group PYR ($P^*<0.05$) and significant different between Groups CON and SAL from Group PYR, respectively ($^{**}P<0.01$).

ATPase activity

The adenosine triphosphatase (ATPase) activity was reduced in all three suspension groups relative to Group CON. ATPase activities (μmol/mgprot/h) in Groups SUS and SAL were decreased by 57% and 59% from Group CON, respectively. However, they were 42% and 51% higher in the PYR group than in the SUS and SAL groups, respectively. There were statistically significant differences between the SUS and SAL groups from the CON and PYR groups ($P<0.01$; Fig. 7 B). But, the ATPase activity in Group PYR was still significantly reduced relative to Group CON ($P<0.01$).

The ATPase activity was reduced in all three suspension groups. There were statistically significant differences between the SUS and SAL groups from the CON and PYR groups. But, the ATPase activity in Group PYR was still significantly reduced relative to Group CON. There were statistically significant differences between Groups CON, SUS and SAL from Group PYR, respectively ($^{**}P<0.01$).

The rats' diet, defecation and general activity in the experiment were normal, no tail injury and death occurred.

Discussion

Major findings and interpretation

Morphological changes

As demonstrated previously [3,8], present results further showed that the microgravity in Groups SUS and SAL led to significant morphological changes in L5 DRG neurons in rats, while the cell features of the

PYR group were almost undistinguishable from those in the CON group without HU experienced in HE staining (Fig. 1). The Nissl body is composed of neurons' rough endoplasmic reticulum (ER) and free polyribosomes. Its alterations of functional status and morphology can reflect neuron's activities in synthesis of proteins and relevant nutritional factors and its survival [18,19]. Results discovered that the impairment of Nissl stained neurons in Groups SUS and SAL was serious, while changes in Group PYR were slight, compared to Group CON under a light microscope (Fig. 2 A and B). Further, alterations in immunofluorescence of dgen-MBP in L5 DRG and L5 spinal cord scan were in parallel with changes above in various groups following the 8-week HU in rats (Fig. 3 A and B; Fig. 4 A and B).

These data first evidenced that HU-induced microstructure damage in DRG could be significantly alleviated by oral pyruvate. Oral pyruvate protected Nissl body from HU injury was supported by recent findings that pyruvate inhibited ER stress in high glucose, *in vitro* (Accepted, FEBS Open Bio, 2020). Notably, an analogical protection of Nissl staining in motor neurons by ethyl pyruvate (EP, a derivate of sodium pyruvate) in spinal cord ischemia reperfusion injury was also reported recently [20].

Functional changes

GDNF has a strong neurotrophic effect on spinal motor neurons in prevention of their degeneration and can rescue cells from apoptosis as well as their death following injury. When nerve damage occurs, the GDNF content can be altered with early stimulated increase following by subsequent decline [21,22]. As previously reported that DRG injury induced GDNF reduction [8, 23,24], the results here showed that relative GDNF proteins in Groups SUS and SAL were significantly decreased, compared with those in Groups CON and PYR following an 8-week HU. In contrary, the GDNF expression in Group PYR was accumulated surprisingly to over 2-fold of those in Groups SUS and SAL, even much more than that in Group CON. The results of GDNF mRNA detection in the groups were also comparable with changes above (data not shown) [25]. The results evidently showed that the DRG injury at the early stage had a prominent feedback increase of GDNF protein with pyruvate supplementation daily (Fig. 5). The underlying causes of profoundly enhanced GDNF protein by pyruvate are unknown at present. To our best knowledge, there has been no report regarding the pyruvate stimulation of GDNF expression, *in vivo*, though EP also showed a mimic effect in primary astrocyte cultures, *in vitro* [26]. Interestingly, it has been known that histone deacetylase inhibitors (HDACi), like sodium butyrate, up-regulate GDNF gene transcription in astrocytes to protect dopaminergic neurons, via HDAC inhibition [27], and pyruvate is one of HDACis [28,29]. Nevertheless, it is first revealed that oral pyruvate can robustly promote the secretion of GDNF that attenuates DRG damage during HU. Currently, exogenous GDNF is suitable for SCI treatment [30,31]. Thus, it is assumed that more benefits may be targeted with pyruvate addition in a novel GDNF combination intervention for SCI treatment.

GFAP is a unique cytoskeleton protein in astrocytes of DRG, the main component of intermediate filament network that warrants cell integrity and resilience. It is considered a sign of the maturation of astrocytes and mainly involved in the structure and metabolism of neurons, but rarely expressed in physiological conditions [32]. Results here showed that relative GFAP expressions were significantly increased in

Groups SUS and SAL (Fig. 6), indicating that astrocytes were activated in DRG injury and the predominant expression of GFAP might be associated with the repairment of DRG damage. It was significantly declined in Group PYR than in both Groups SUS and SAL, but still raised relative to Group CON. These data demonstrated that oral pyruvate could provide the neuroprotective effect on damaged DRG in the early HU injury, as previously indicated that pyruvate could limit or better control the reactive astrocyte proliferation (gliosis) and sustain the morphological integrity of injured astrocytes [9,33]. Also, GFAP mRNA detection showed changes in the groups in a similar manner (data not shown). However, current pyruvate dosage could not fully prevent the damage. Again, EP was reported to attenuate its expression in astrocytes in rats with ischemic spinal cord [34].

Intriguingly, GDNF is reductive of astrogliosis, as early found that GDNF promoted the spinal cord graft survival and growth, but reduced GFAP immunoreactivity [35,36]. Present results first demonstrated that oral pyruvate upregulated the former and attenuated the later in DRG nerves during HU. These results suggest that GDNF and GFAP as well as pyruvate play a pivotal role in maintaining environmental stability, neuronal survival and plasticity repair in the nervous system [32].

The levels of ATP and ATPase in Groups SUS and SAL were significantly decreased relative to those in Groups CON and PYR (Fig. 7 A and B). Results evidenced that cellular energy metabolism was declined by HU injury and oral pyruvate in Group PYR profoundly preserved energy metabolism in DRG nerves during the period of microgravity, so that nerve tissues' structure and function were mostly protected. Although ATP and ATPase levels in Group PYR were relatively preserved, they were still significantly inferior to those in Group CON. Metabolic studies reveal that glycolysis is usually stimulated with inhibition of glucose oxidative phosphorylation in microgravity conditions [37]. Blood pyruvate, as pyruvate dehydrogenase kinase (PDK) inhibitor like dichloroacetate (DCA), can easily enter mitochondria of nervous cells, activate the depressed pyruvate dehydrogenase (PDH) via PDK inhibition to even full context and promote the tricarboxylic acid (TCA) cycle metabolism [35,38,39], though the PDH activity was not detected here (see below). Further, its anti-oxidative stress and anti-inflammation may simultaneously benefit in TCA cycle function in addition as an important energetic substrate [10,13,40]. As a result, ATP production and ATPase activity were significantly preserved in Group PYR.

In all, these results discovered that Group PYR showed morphological alterations close to Group CON, while the energy metabolic disorder and cell dysfunction were strikingly attenuated by oral pyruvate, but not fully recovered with current pyruvate dosage from the HU injury. The reason of divergence between histological and functional changes was not clear at present. The dose-effect curve remains explored.

Oral pyruvate implication in space flight

Present results provide additional evidence with 0.55% pyruvate that a low oral pyruvate (0.33-4% in drink water) does protect the structure and function of nerve systems [13,41-44]. Thus, oral pyruvate may be useful in attenuation or prevention of DRG, SCI and other disorders for astronauts in space missions.

The dose of oral pyruvate (0.55%) in the experiment was empirically chosen and the ideal concentration and optimal dosage of oral pyruvate solution for astronauts remain explored. Notably, oral or intravenous (IV) pyruvate in large dosages has been reported in several preliminary clinical trials with safety and effectiveness in absence of clinical toxicity [45-49]. However, oral ingestion of small doses of pyruvate alone does not elevate plasma pyruvate, but a large dosage is of gastrointestinal irritation in humans 45,50]. On the other hand, the novel pyruvate solution (Pyr-ORS): equimolar pyruvate replacement of bicarbonate or citrate in the World Health Organization-guided ORS (WHO-ORS) [51], containing 0.35% pyruvate and 1.35% glucose as an experimental drink water, effectively preserved neurons structure and function in hippocampal CA1 regions following asphyxial cardiac arrest in rats [13]. Further, Pyr-ORS and 1% pyruvate as drink water comparably showed a robust PDH activity renovated and blood sugar and kidney function preserved in diabetic *db/db* mice [52].

Several animal studies strongly indicate that around 10.0g of oral sodium pyruvate daily as a functional drink in a formula as Pyr-ORS may be beneficial and feasible for astronauts in space flights due to Na^+-Glucose co-transporter existed in intestinal epithelium in mammalian [13,42,51]. As to metabolic profile of post-pyruvate, it was recently illustrated [53,54]. Further studies are required and the clinical trials with Pyr-ORS formula, modified if needed, are warranted in astronauts' training ground and in general SCI treatment.

Finally, it has to be pointed out that although EP showed the protection of nervous system [20,26,34], there is a distinct difference between them: EP does not work in humans [54], leading to its clinical perspective hopelessly.

Limitations

1) Present data focused on a principal proof, *in vivo*, for oral pyruvate protection in rats subjected to HU injury. Nevertheless, cell experiments, *in vitro*, to demonstrate the direct effect of pyruvate on DRG nerve cells following weightlessness would further support the hypothesis and explore the underlying molecular mechanisms of the pyruvate action. 2) If double immunofluorescence with anti-neurofilament antibody in addition to dgen-MBP expression was performed, the MBP pictures would be more visible with pyruvate treatment. 3) Oral pyruvate in Pyr-ORS (0.35%) was not compared in the experiment; to establish a dose-response manner would further illustrate oral pyruvate effects on DRG in rats subjected to microgravity.

Conclusion

Hindlimb unweighting resulted in significant L5 DRG damage in both tissue morphology and cell function in rats. Present results first demonstrate that oral pyruvate can effectively protect the DRG tissues against HU injury. The optimal dosage of oral pyruvate and pyruvate formula remain explored for astronauts' use in space missions.

Abbreviations

ATP, Adenosine triphosphate; ATPase, Adenosine triphosphatase; dgen-MBP, degenerated myelin basic protein; DRG, Dorsal root ganglia; GDNF, Glial cell line-derived neurotrophic factor; GFAP, Glial fibrillary acidic protein; HU, Hindlimb unweighting; L5, lumbar 5

Declarations

Ethics approval and consent to participate

All protocols in this study were approved by the Guidelines of Animal Testing Committee of the PLA General Hospital, Beijing, China. The animal care and treatment procedures were in line with Guiding Principles for Animal Care and Use in the Department of Physiology and Sciences, Beijing, China.

Consent for publication

Not applicable.

Availability of data and materials

Data and materials can be provided upon requests.

Competing interests

The authors declare no conflict of interests.

Funding

Supported by the Foundation of State Key Lab of Space Medicine Fundamentals and Application, China (SMFA15K03); the fund was received by Dr. Cui G. The fund provider did not participate in the experimental design, conduction, data analysis, explanation, discussion and sending for publication.

Authors' contribution

Zhou FQ, Cui G and Li Y designed the experiment; Li Y, Zhang H, Ren NT, Chen C and Qi P performed the animal studies, collected the data and analyzed the results; Li Y and Zhou FQ wrote the manuscript and Zhou FQ and Cui G critically revised the manuscript.

Acknowledgements

Not applicable

ARRIVE Guidelines checklist

All sections of this study are following the ARRIVE Guidelines for animal research (PLoS Biol. 2020;8:e1000412). A checklist of completed ARRIVE guidelines is included in supplementary file.

References

1. 1
   1., Trappe S, Costill D, Gallagher P, Creer A, Peters JR, Evans H, Riley DA, Fitts RH. Exercise in space: human skeletal muscle after 6 months aboard the International Space Station. J Appl Physiol (1985). 2009;106:1159-68.
2. 2., Chang DG, Healey RM, Snyder AJ, Sayson JV, Macias BR, Coughlin DG, Bailey JF, Parazynski SE, Lotz JC, Hargens AR. Lumbar spine paraspinal muscle and intervertebral disc height changes in astronauts after long-duration spaceflight on the international space station. Spine (Phila Pa 1976). 2016;41:1917–24.
3. 3., Zhang R, Ran HH, Cai LL, Zhu L, Sun JF, Peng L, Liu XJ, Zhang LN, Fang Z, Fan YY, Cui G. Simulated microgravity-induced mitochondrial dysfunction in rat cerebral arteries. FASEB J. 2014;28:2715–24.
4. 4., Kennedy AR, Crucian B, Huff JL, Klein SL, Morens D, Murasko D, Nickerson CA, Sonnenfeld G. Effects of sex and gender on adaptation to space: immune system. J Womens Health (Larchmt). 2014;23:956–8.
5. 5., Islamov RR, Rizvanov AA, Tyapkina OV, Shenkman BS, Kozlovskaya IB, Nikolskiy EE, Grigoryev AI. Genomic study of gene expression in the mouse lumbar spinal cord under the conditions of simulated microgravity. Dokl Biol Sci. 2011;439:197–200.
6. 6., Zhang R, Ran HH, Ma J, Bai YG, Lin LJ. NAD(P)H oxidase inhibiting with apocynin improved vascular reactivity in tail-suspended hindlimb unweighting rat. J Physiol Biochem. 2012;68:99–105.
7. 7., Falcai MJ, Zamarioli A, Leoni GB, de Sousa Neto MD, Volpon JB. Swimming activity prevents the unloading induced loss of bone mass, architecture, and strength in rats. Biomed Res Int. 2015;2015:507848.
8. Zhang 8, Ren H, Zhou NT, Li FQ, Lei J, Liu W, Bi N, Wu L, Zhang ZX, Zhang R, Cui YG. G. Effects of hindlimb unweighting on MBP and GDNF expression and morphology in rat dorsal root ganglia neurons. Neurochem Res. 2016;41:2433–42.
9. 9., Sharma P, Karian J, Sharma S, Liu S, Mongan PD. Pyruvate ameliorates post ischemic injury of rat astrocytes and protects them against PARP mediated cell death. Brain Res. 2003;992:104–13.
10. Hu 10, Liu S, Zhao WW, Lin Y, Luo ZL, Bai HM, Sheng XD, Zhou ZY. FQ. Pyruvate-enriched oral rehydration solution improved intestinal absorption of water and sodium during enteral resuscitation in burns. Burns. 2014;40:693–701.
11. 11., Hu S, Dai YL, Gao MJ, Wang XN, Wang HB, Dou YQ, Bai XD, Zhou FQ. Pyruvate as a novel carrier of hydroxyethyl starch 130/0.4 may protect kidney in rats subjected to severe burns. J Surg Res. 2018;225:166–74.
12. 12., Gruenbaum BF, Kutz R, Zlotnik A, Boyko M. Blood glutamate scavenging as a novel glutamate-based therapeutic approach for post-stroke depression. Ther Adv Psychopharmacol. 2020 Feb 17;10:2045125320903951. doi:10.1177/2045125320903951.

13. 13., Bai W, Li J, Han R, Ying G, Sun X, Jing Y, Zhou F, Gao C. Effects of hypotonic pyruvate oral rehydration solution on brain injury in rats subjected to asphyxial cardiac arrest. Chinese J Injury Repair Wound Healing. 2017;12:326–30 (in Chinese with English abstract).
14. 14
14., Han Q, Xiang J, Zhang Y, Qiao H, Shen Y, Zhang C. Enhanced neuroprotection and improved motor function in traumatized rat spinal cords by rAAV2-mediated glial-derived neurotrophic factor combined with early rehabilitation training. Chin Med J (Engl). 1998;2014;127:4220-5.
15. 15., Goudemant JF, Van Beers BE, Demeure R, Grandin C, Delos M, Pringot J. Comparison of unenhanced and gadoxetate disodium-enhanced spin-echo magnetic resonance imaging for the detection of experimental hepatocellular carcinoma in the rat. Invest Radiol. 1998;33:80–4.
16. 16., Weicker H, Hageloch W, Luo J, Müller D, Werle E, Sehling KM. Purine nucleotides and AMP deamination during maximal and endurance swimming exercise in heart and skeletal muscle of rats. Int J Sports Med. 1990;11 Suppl 2:68–77.
17. 17., Bando Y, Nomura T, Bochimoto H, Murakami K, Tanaka T, Watanabe T, Yoshida S. Abnormal morphology of myelin and axon pathology in murine models of multiple sclerosis. Neurochem Int. 2015;81:16–27.
18. 18., Johnson IP, Sears TA. Target-dependence of sensory neurons: an ultrastructural comparison of axotomised dorsal root ganglion neurons with allowed or denied reinnervation of peripheral targets. Neuroscience. 2013;228:163–78.
19. 19., Luo L, Li C, Deng Y, Wang Y, Meng P, Wang Q. High-Intensity interval training on neuroplasticity, balance between brain-derived neurotrophic factor and precursor brain-derived neurotrophic factor in poststroke depression rats. J Stroke Cerebrovasc Dis. 2019;28:672–82.
20. 20., Nguyen BN, Albadawi H, Oklu R, Crawford RS, Fink MP, Cambria RP, Watkins MT. Ethyl pyruvate modulates delayed paralysis following thoracic aortic ischemia reperfusion in mice. J Vasc Surg. 2016;64:1433–43.
21. 21., Satake K, Matsuyama Y, Kamiya M, Kawakami H, Iwata H, Adachi K, Kiuchi K. Up-regulation of glial cell line-derived neurotrophic factor (GDNF) following traumatic spinal cord injury. Neuroreport. 2000;11:3877–81.
22. 22., Hara T, Fukumitsu H, Soumiya H, Furukawa Y, Furukawa S. Injury-induced accumulation of glial cell line-derived neurotrophic factor in the rostral part of the injured rat spinal cord. Int J Mol Sci. 2012;13:13484–500.
23. 23., Nagano M, Sakai A, Takahashi N, Umino M, Yoshioka K, Suzuki H. Decreased expression of glial cell line-derived neurotrophic factor signaling in rat models of neuropathic pain. Br J Pharmacol. 2003;140:1252–60.
24. 24., Miyazaki H, Nagashima K, Okuma Y, Nomura Y. Expression of glial cell line-derived neurotrophic factor induced by transient forebrain ischemia in rats. Brain Res. 2001;922:165–72.
25. 25., Tsybko AS, Ilchibaeva TV, Kulikov AV, Kulikova EA, Krasnov IB, Sychev VN, Shenkman BS, Popova NK, Naumenko VS. Effect of microgravity on glial cell line-derived neurotrophic factor and cerebral

dopamine neurotrophic factor gene expression in the mouse brain. J Neurosci Res. 2015;93:1399–404.

26. 26., Shin JH, Kim SW, Jin Y, Kim ID, Lee JK. Ethyl pyruvate-mediated Nrf2 activation and hemeoxygenase 1 induction in astrocytes confer protective effects via autocrine and paracrine mechanisms. Neurochem Int. 2012;61:89–99.
27. 27., Wu X, Chen PS, Dallas S, Wilson B, Block ML, Wang CC, Kinyamu H, Lu N, Gao X, Leng Y, Chuang DM, Zhang W, Lu RB, Hong JS. Histone deacetylase inhibitors up-regulate astrocyte GDNF and BDNF gene transcription and protect dopaminergic neurons. Int J Neuropsychopharmacol. 2008;11:1123–34.
28. 28., Thangaraju M, Gopal E, Martin PM, Ananth S, Smith SB, Prasad PD, Sterneck E, Ganapathy V. SLC5A8 triggers tumor cell apoptosis through pyruvate-dependent inhibition of histone deacetylases. Cancer Res. 2006;66:11560–4.
29. 29., Spiegel S, Milstien S, Grant S. Endogenous modulators and pharmacological inhibitors of histone deacetylases in cancer therapy. Oncogene. 2012;31:537–51.
30. 30., Ortmann SD, Hellenbrand DJ. Glial cell line-derived neurotrophic factor as a treatment after spinal cord injury. Neural Regen Res. 2018;13:1733–4.
31. 31
    10.3390/brainsci8060109
    31., Walker MJ, Xu XM. History of glial cell line-derived neurotrophic factor (GDNF) and its use for spinal cord injury repair. Brain Sci. 2018;8 pii: E109. doi:10.3390/brainsci8060109.
32. 32., Middeldorp J, Hol EM. GFAP in health and disease. Prog Neurobiol. 2011;93:421–43.
33. 33., Rouleau C, Rakotoarivelo C, Petite D, Lambert K, Fabre C, Bonardet A, Mercier J, Baldet P, Privat A, Langley K, Mersel M. Pyruvate modifies glycolytic and oxidative metabolism of rat embryonic spinal cord astrocyte cell lines and prevents their spontaneous transformation. J Neurochem. 2007;100:1589–98.
34. 34., Djedović N, Stanisavljevic S, Jevtić B, Momčilović M, Lavrnja I, Miljković D. Anti-encephalitogenic effects of ethyl pyruvate are reflected in the central nervous system and the gut. Biomed Pharmacother. 2017;96:78–85.
35. 35., Trok K, Hoffer B, Olson L. Glial cell line-derived neurotrophic factor enhances survival and growth of prenatal and postnatal spinal cord transplants. Neuroscience. 1996;71:231–41.
36. 36., Iannotti C, Li H, Yan P, Lu X, Wirthlin L, Xu XM. Glial cell line-derived neurotrophic factor-enriched bridging transplants promote propriospinal axonal regeneration and enhance myelination after spinal cord injury. Exp Neurol. 2003;183:379–93.
37. 37., Michaletti A, Gioia M, Tarantino U, Zolla L. Effects of microgravity on osteoblast mitochondria: a proteomic and metabolomics profile. Sci Rep. 2017;7:15376.
38. doi: 10.1038/s41598-017-15612-1.
39. 38., Priestman DA, Orfali KA, Sugden MC. Pyruvate inhibition of pyruvate dehydrogenase kinase. Effects of progressive starvation and hyperthyroidism in vivo, and of dibutyryl cyclic AMP and fatty

acids in cultured cardiac myocytes. FEBS Lett. 1996;393:174–8.

40. , Kuzmiak-Glancy JR 3rd, Brooks S, Swift DM, LM, Posnack NG, Kay. MW.
41. Functional response of. the isolated, perfused normoxic heart to pyruvate dehydrogenase activation by dichloroacetate and pyruvate. Pflugers Arch. 2016;468:131–42.
42. 40., Sharma P, Benford B, Li ZZ, Ling GS. Role of pyruvate dehydrogenase complex in traumatic brain injury and measurement of pyruvate dehydrogenase enzyme by dipstick test. J Emerg Trauma Shock. 2009;2:67–72.
43. , Sahenk Z, Yalvac ME, Amornvit J, Arnold WD, Chen L, Shontz KM, Lewis S. Efficacy of exogenous pyruvate in Trembler^{J} mouse model of Charcot-Marie-Tooth neuropathy. Brain Behav. 2018;8:e01118. doi:10.1002/brb3.1118.
44. , Koivisto H, Leinonen H, Puurula M, Hafez HS, Barrera GA, Stridh MH, Waagepetersen HS, Tiainen M, Soininen P, Zilberter Y, Tanila H. Chronic pyruvate supplementation increases exploratory activity and brain energy reserves in young and middle-aged mice. Front Aging Neurosci. 2016;8:41. doi:10.3389/fnagi.2016.00041.
45. 43., Qi YX, Fu JD, Wang YQ, Wang DL. Effects of pyruvate on retinal oxidative damage and retinal ultrastructure in diabetic rats. Int Eye Sci. 2014;14:2143–6.
46. 44., Zilberter M, Ivanov A, Ziyatdinova S, Mukhtarov M, Malkov A, Alpár A, Tortoriello G, Botting CH, Fülöp L, Osypov AA, Pitkänen A, Tanila H, Harkany T, Zilberter Y. Dietary energy substrates reverse early neuronal hyperactivity in a mouse model of Alzheimer's disease. J Neurochem. 2013;125:157–71.
47. 45., Petkova I, Hristov V, Petrov K, Thorn W. Oral application of sodium pyruvate in healthy persons and patients with diabetes mellitus type I. Comptes rendus de l’Acad´emie bulgare des Sciences. 2007;60:579–84.
48. 46., Koga Y, Povalko N, Inoue E, Nashiki K, Tanaka M. Biomarkers and clinical rating scales for sodium pyruvate therapy in patients with mitochondrial disease. Mitochondrion. 2019;48:11–5.
49. 47., Mateva L, Petkova I, Petrov K, Beniozef D, Bojilova M, Vankova L, Thorn W. Ten-day course of sodium pyruvate infusions in patients with chronic liverdiseases (CLD). Jpn Pharmacol Ther. 1996;24:115–25.
50. 48., Schillinger W, Hünlich M, Sossalla S, Hermann H-P, Hasenfuss G. Intracoronary pyruvate in cardiogenic shock as an adjunctive therapy to catecholamines and intra-aortic balloon pump shows beneficial effects on hemodynamics. Clin Res Cardiol. 2011;100:433–8.
51. 49., Van Erven P, Gabreels F, Wevers R, Doesburg W, Ruitenbeek W, Renier W, Lamers K. Intravenous pyruvate loading test in Leigh syndrome. J Neurol Sci. 1987;77:217–27.
52. 50., Morrison MA, Spriet LL, Dyck DJ. Pyruvate ingestion for 7 days does not improve aerobic performance in well-trained individuals. J Appl Physiol. 2000;89:549–56.
53. 51., Liu R, Wang SM, Li ZY, Yu W, Zhang HP, Zhou FQ. Pyruvate in reduced osmolarity oral rehydration salt corrected lactic acidosis in sever scald rats. J Surg Res. 2018;226:173–80.

54. 52., Zhang XM, Wang YZ, Tong JD, Ning XC, Zhou FQ, Yang XH, Jin HM. Pyruvate alleviates high glucose-induced endoplasmic reticulum stress and apoptosis in HK-2 cells. FEBS Open Bio. 2020 Mar 9. doi:10.1002/2211-5463.12834.
55. 53., Hu S, Xiao DB, Xian QL, Hai BW, Yu XZ, Fang T, Zhou FQ. Pyruvate Ringer's solution corrects lactic acidosis and prolongs survival during hemorrhagic shock in rats. J Emerg Med. 2013;45:885–93.
56. 54., Zhou FQ. Pyruvate research and clinical application outlooks a revolutionary medical advance. Int J Nutr. 2020;5:1–8.

Figures

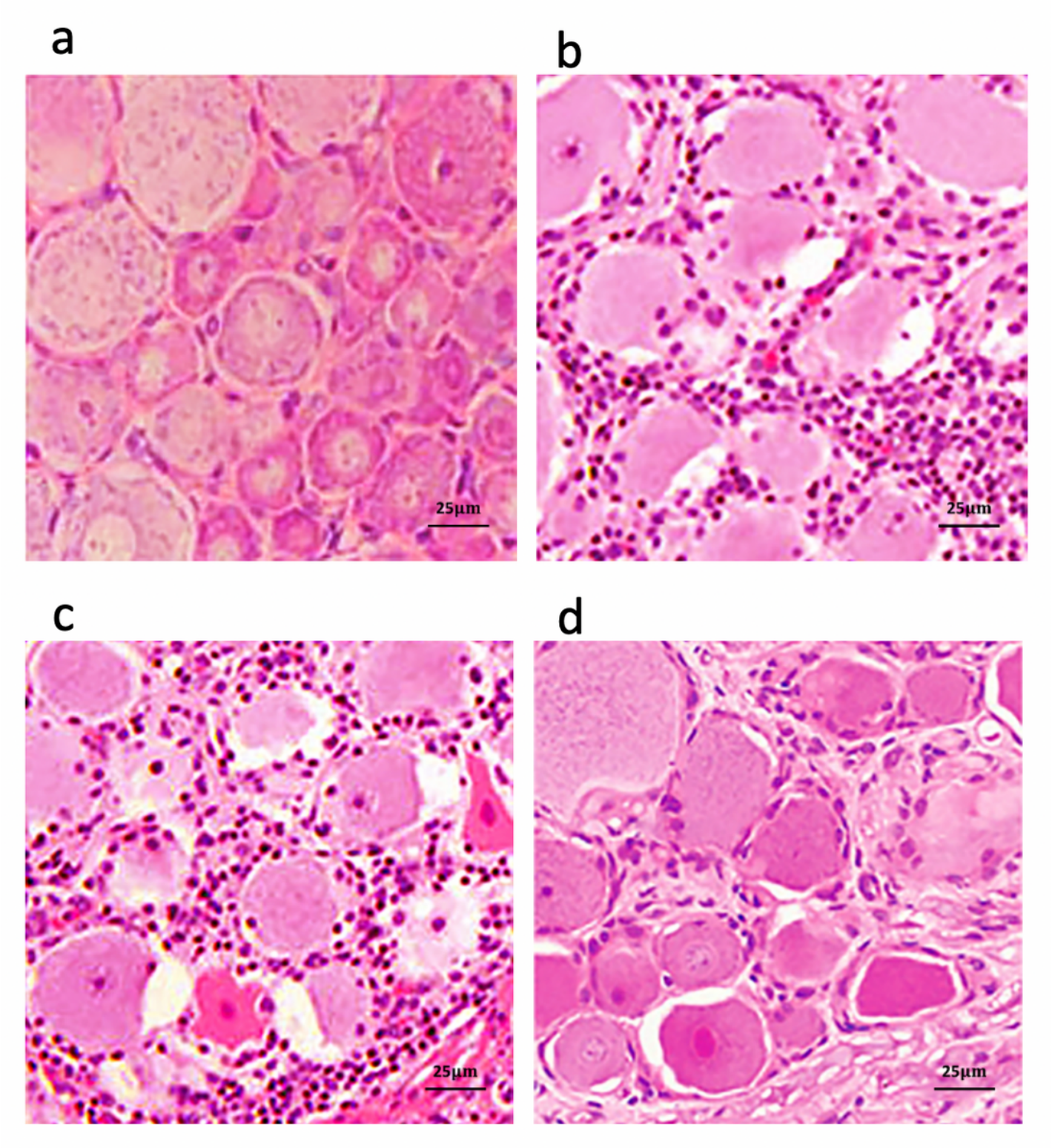

Figure 1

Hematoxylin-Eosin (HE) staining of L5 DRG tissues in various treatment groups

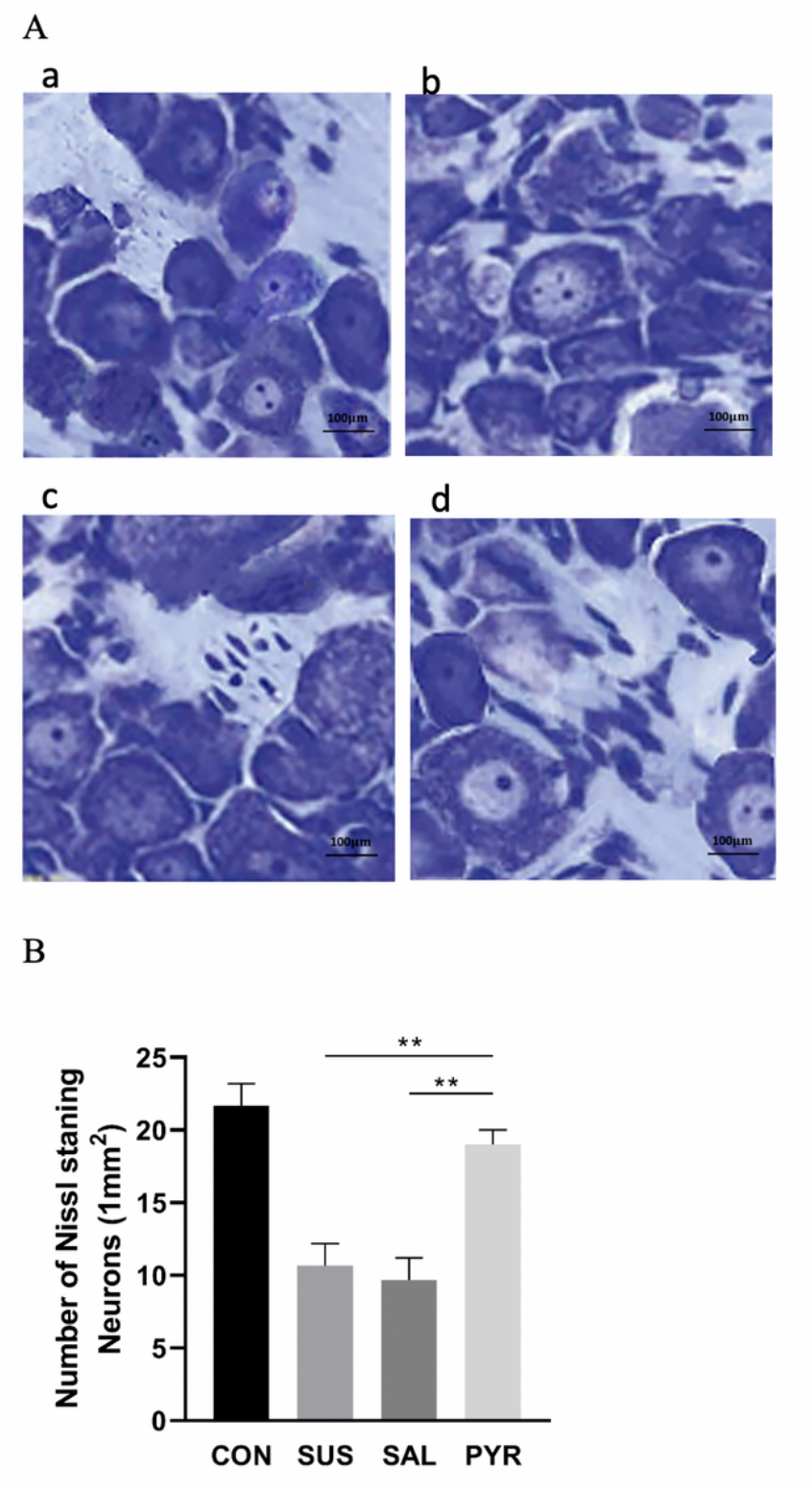

Figure 2

Fig. 2 A. Toluidine blue staining of Nissl bodies in L5 DRG neurons in various treatment groups Fig. 2 B. Quantified analysis of Nissl body staining in various treatment groups

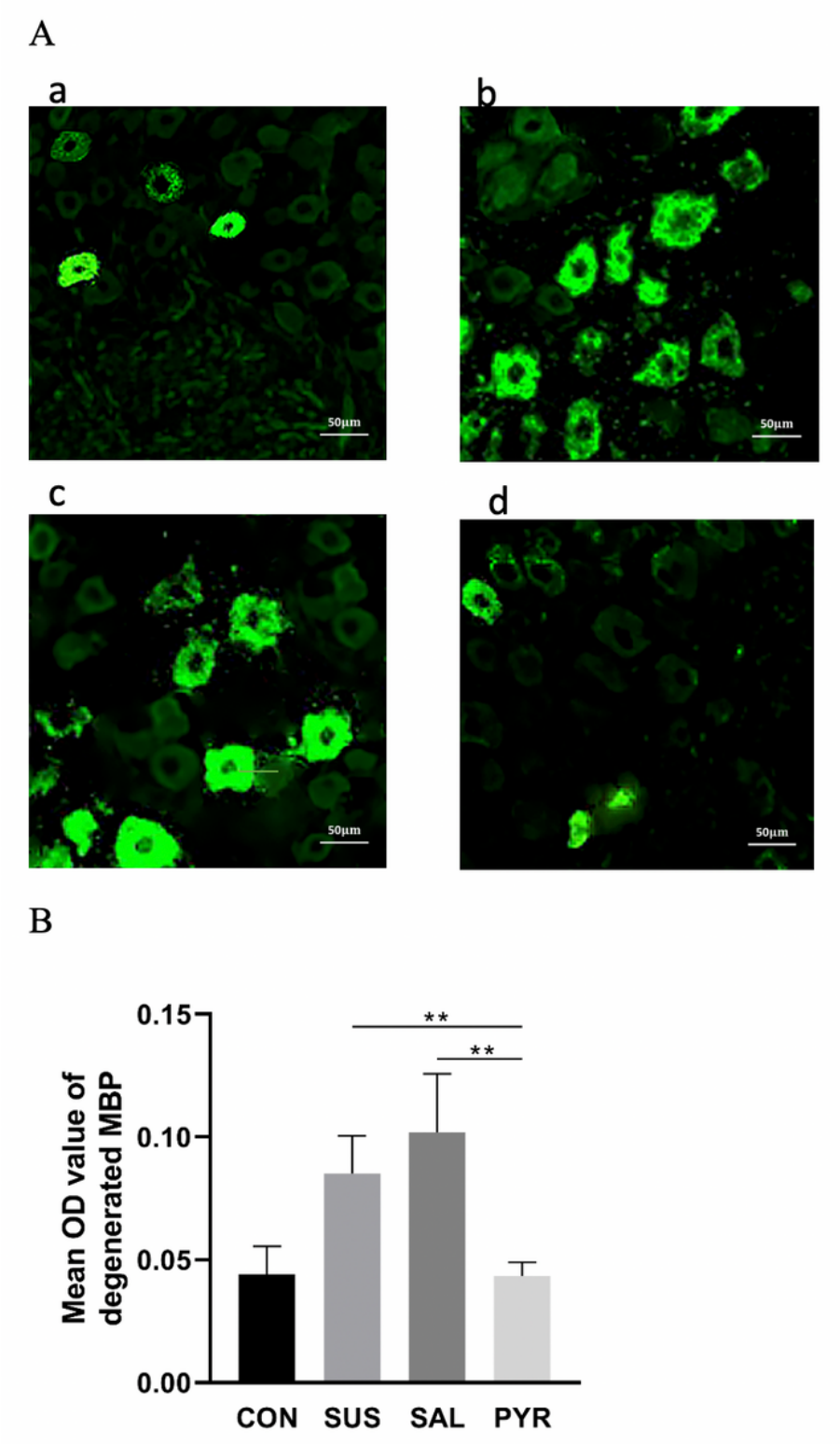

Figure 3

Fig. 3 A. Immunofluorescence detection of L5 DRG dgen-MBP in various treatment groups Fig. 3 B. Mean OD value of dgen-MBP in various treatment groups

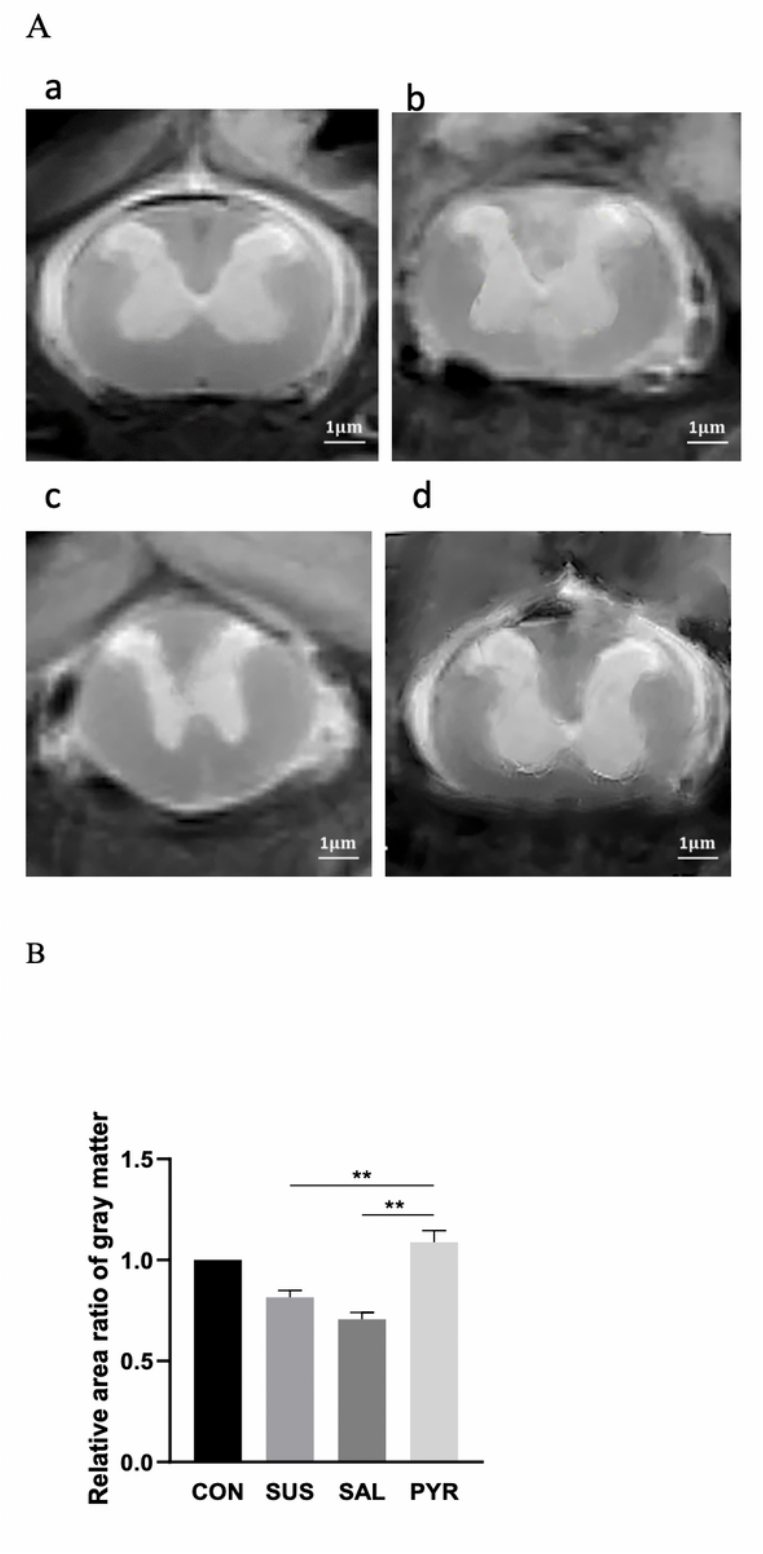

Figure 4

Fig. 4 A. The areas of gray matter and white matter in the L5 spinal cord in various treatment groups Fig. 4 B. The relative area ratio of gray matter in various treatment groups

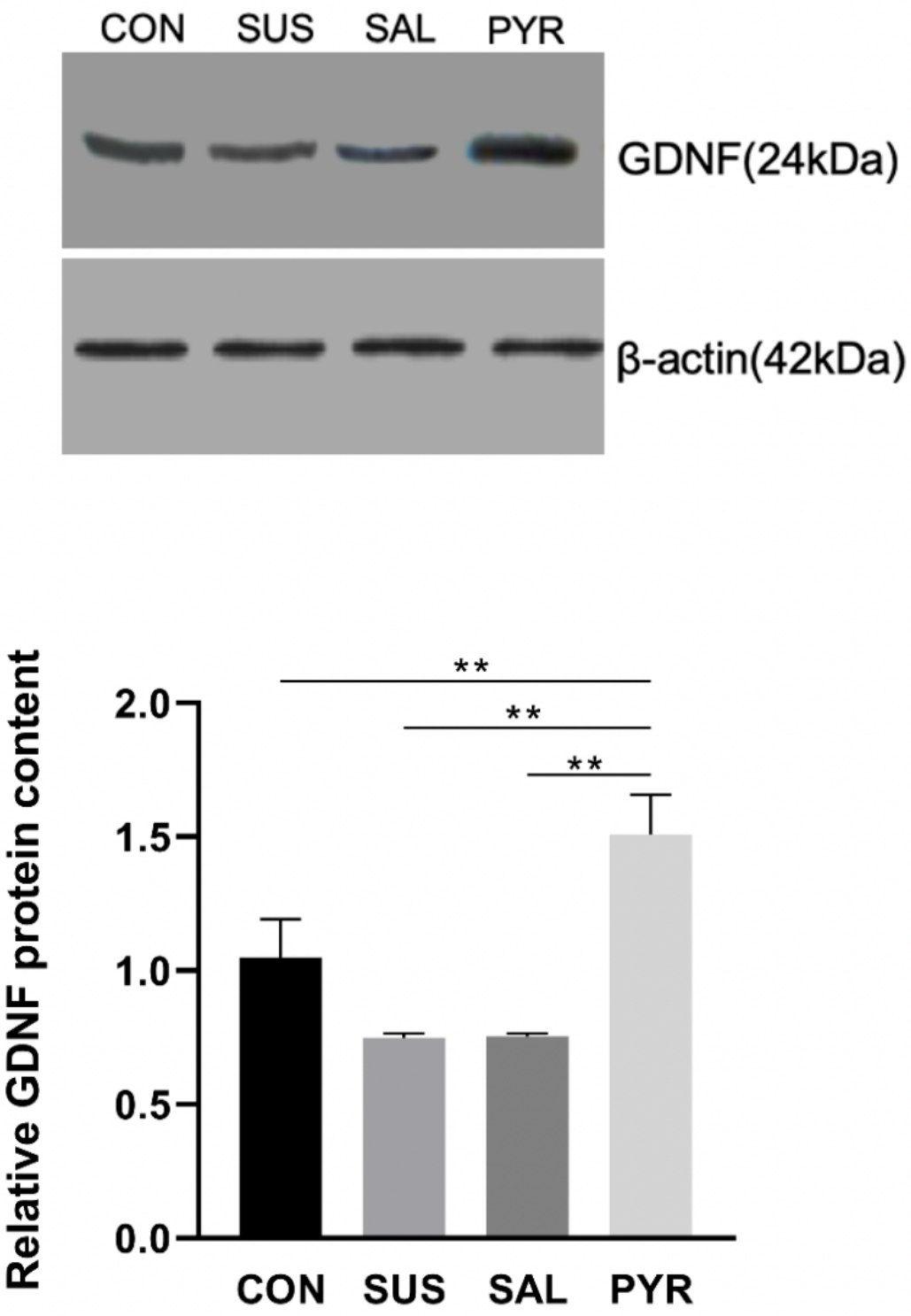

Figure 5

Relative GDNF expressions by Western blotting in L5 DRG neurons in various treatment groups

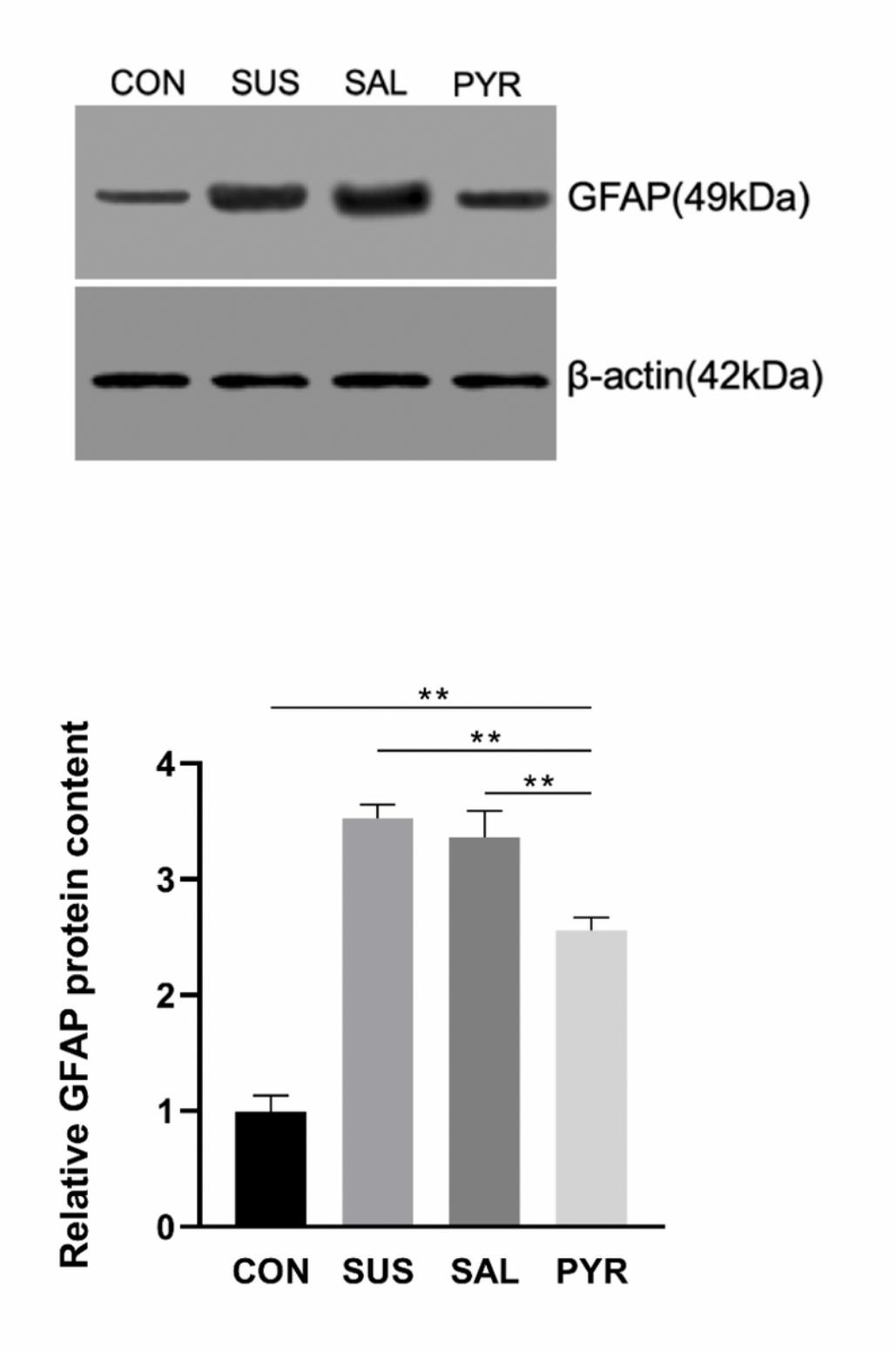

Figure 6

Relative GFAP expressions by Western blotting in L5 DRG tissues in various treatment groups

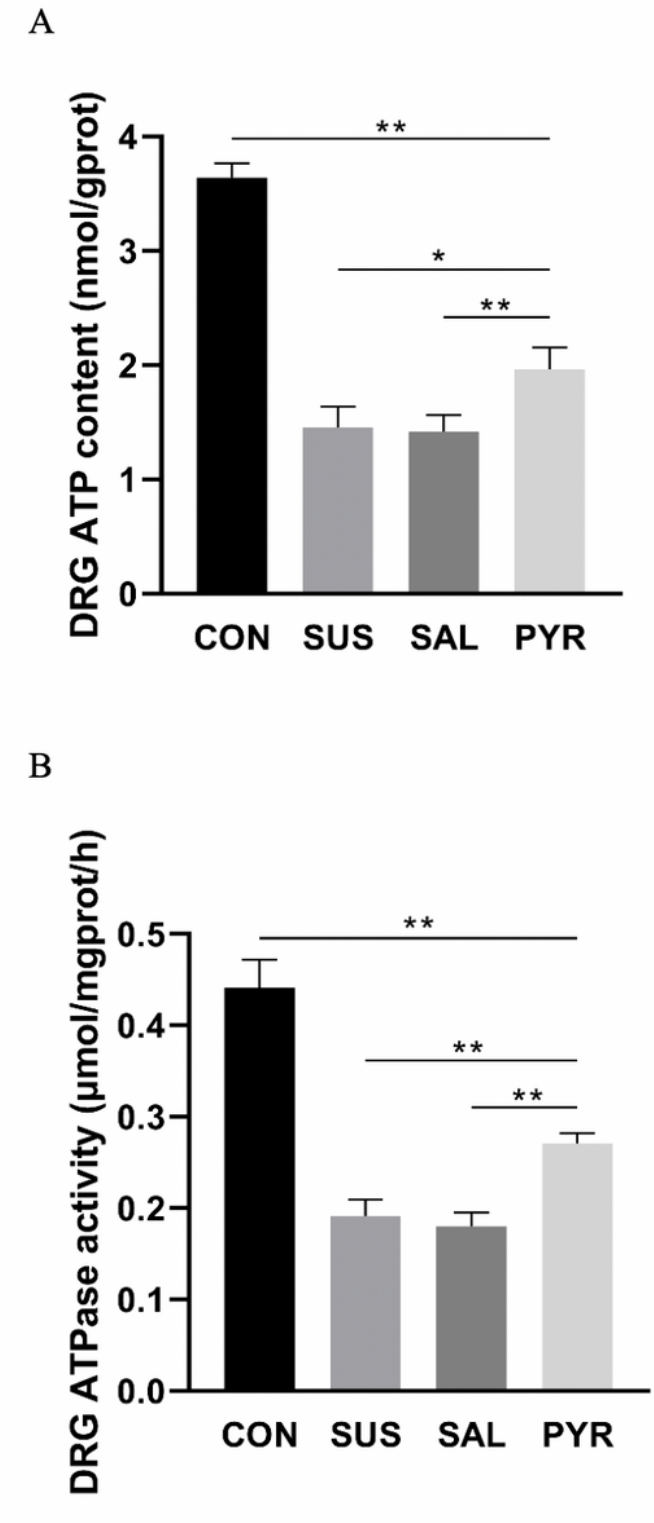

Figure 7

Fig. 7 A. ATP contents in L5 DRG tissues in various treatment groups Fig. 7 B. ATPase activities in L5 DRG tissues in various treatment groups